J. Meier, S. Rudolph, T. Schanz: Effective Algorithm for parameter back calculation - Geotechnical Applications
published in: Bautechnik Volume 86 Issue S1, Pages 86 - 97

Effective Algorithm for parameter back calculation – Geotechnical Applications

Jörg Meier[1], Sebastian Rudolph[2], Tom Schanz[3]

Abstract:

When working with numerical models, it is essential to determine model parameters which are as realistic as possible. Optimization techniques are used more and more frequently to solve this task. However, using these methods may lead to very high time costs – in particular, if rather complicated forward calculations are involved. In this paper, we present a class of methods whitch allows estimating the solution of this kind of optimization problems based on relatively few sampling points. We put very weak constraints on the sampling point distribution; hence, they may be taken from previous forward calculations as well as from alternative sources.

Starting from an introduction into the theoretical approach, a strategy for speeding up inverse optimization problems is introduced which is illustrated by an example from geomechanics.

1 Introduction and Motivation

For determining model parameters, several strategies are available. On one side, these parameter values can be identified on the basis of field and laboratory tests. However, this strategy usually requires extensive time and financial resources. On the other side, values from literature and empirical values can be used, if applicable. Admittedly, these values have to be considered as imprecise. As a third possibility, a parameter back calculation by means of an iterative adjustment can be used. In this approach, the resulting system response of a simulation is compared to real measurements. By an iterative adjustment of the underlying parameters, the simulation result is then successively fitted to the measurements. This approach uses optimization strategies known from applied mathematics.

Parameter back calculation methods are used in more and more application fields. This observation is reflected in the available technical literature: A variety of contributions can be

[1] Dr. Jörg Meier, Gruner AG, Gellertstrasse 55, CH-4020 Basel, Switzerland. Formerly: Laboratory of Soil Mechanics, Bauhaus- Universität Weimar, Coudraystrasse 11c, 99421 Weimar, Germany. joerg.meier@vint.de

[2] Dr. Sebastian Rudolph, Institut AIFB, Universität Karlsruhe, 76128 Karlsruhe, Germany. sebastian.rudolph@kit.edu

[3] Prof. Dr.-Ing. habil. Tom Schanz, Chair and Professor for Foundation Engineering, Soil & Rock Mechanics, Ruhr-Universität Bochum, 44780 Bochum, tom.schanz@ruhr-uni-bochum.de

found e. g. for the subject areas of structural analysis (e. g. MATOUŠ et al. 2000, SCHLEGEL & WILL 2006), mechanical and automotive engineering (e. g. FLORES SANTIAGO & BAUSINGER 1998, FLEISCHER & BROOS 2004), hydrogeology (e. g. BITTERLICH & KNABNER 2002, CARRERA et al. 2005), and fluid mechanics (e. g. FINSTERLE 1998 and 2000, JEONG 2003). A large number of publications on the theoretical foundations and applications can also be found in the mathematical literature (e. g. HADAMARD 1902, BIALY & OLBRICH 1975, LOUIS 1989, SPALL 2003, BOYD & VANDENBERGHE 2006). Applications of optimization procedures in geotechnics were described by many authors, e. g. in the calibration process of geotechnical models (CALVELLO & FINNO 2002 and 2004), or to identify hydraulic parameters from field drainage tests (ZHANG et al. 2003). SCHANZ et al. 2006 applied the Particle Swarm Optimization techniques to geotechnical field projects and laboratory tests, namely a multi-stage excavation and the desaturation of a sand column. Furthermore, MEIER et al. 2008 used the PSO technique for parameter back analysis of a landslide near Corvara in the Dolomites (Italy).

For the iterative adjustment of the parameter values, in many cases a large amount of runs of the simulation ("forward calculation") with different parameter value sets are necessary, often resulting in high runtimes for the overall calculation. In parts, this runtime can be decreased by parallelization of the forward calculations and by speeding up the single simulation steps, but the possible acceleration is limited. Moreover, these options often imply additional costs e. g. new computer equipment for parallelization or working time.

Based on the fact that the necessary calculation effort mainly depends on the number of forward calculations needed, the following objectives for increasing efficiency can be stated:

- *Minimization of total number of forward calculations*: the development towards more and more sophisticated simulations, complex geometries, and constitutive models results in an increase of calculation time required for a single forward calculation. Hence, every saved forward calculation yields a gain of time for the parameter back calculation.
- *Integration of all available and pre-existing information*: The majority of known optimization algorithms only uses information internally calculated. Results of other methods, like pre-existing optimization sequences or statistical analysis are only used rudimentarily or not used at all. For example, a gradient method prescribes the needed parameter value sets while ignoring "outside" data. In line with this objective, the employed optimization methods should preferably be tolerant of the concrete

distribution of the entered parameter-value sets. For example, constraining the input to rastered data only would be unfavorable.

- *Usage of the advantages of known optimization algorithms*: This article is not aimed at developing a novel optimization algorithm. Instead, our intention is rather to benefit from the advantages of known algorithms and to recombine them. Consequently, it makes sense to use interfaces of existing optimization methods to enable the deployment of future and improved algorithms for extreme value determination.

2 Theoretical Background

The chart of the direct approach to the back analysis is shown in Fig. 1. In the basic approach, we choose an objective function $f(x_1, x_2, \ldots, x_n)$ with n parameters to be identified. This function measures the agreement between the available data and the solution of the forward calculation (the model prediction for a given set of parameters). Starting with an initial guess for the parameters, the optimization algorithm invokes the forward calculation once or several times and extracts the relevant data from the solution of the forward problem to be used to determine the according value of f. The associated objective function value is calculated and the procedure continues its search for the set of parameters that minimizes the objective function.

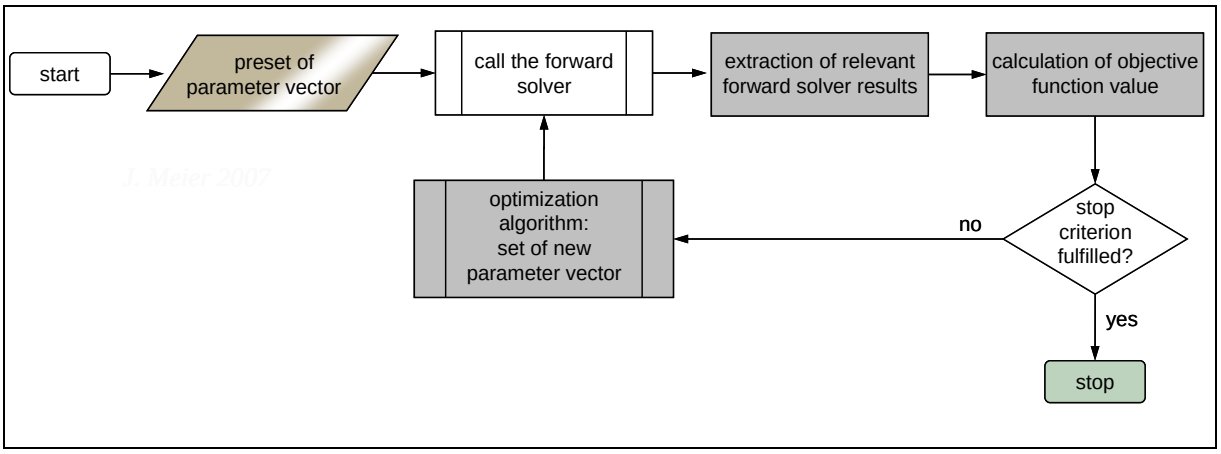

Fig. 1: Basic flowchart for the optimization

To quantify the deviation between the reference data and the model response, the values of the objective function are used. In the literature, many approaches to appropriate objective functions can be found, whereas many are based on the method of least squares. From the mathematical point of view, the n unknown parameters span an n-dimensional search space

wherein a scalar field is defined by the objective function. This scalar field forms an objective function topology. The parameter back calculation can be seen as search for the lowest, respectively highest, point of this topology.

To discuss the numerous optimization algorithms present in the literature is certainly beyond the scope of this paper. Hence we will only review the main categories and their properties in the sequel:

- *Stochastic methods*: The category of stochastic methods comprises algorithms using mainly combinatorial and/or random number based paradigms. Examples are Monte-Carlo sampling, Latin-Hypercube sampling, Metropolis Algorithm, Gibbs Sampler and Simulated Annealing. Clear advantages of those approaches are their robustness and invariance towards rough objective function topologies. Furthermore, many of these algorithms show global characteristics. Among the disadvantages is the relatively low performance with respect to problems with a higher number of unknown variables.
- *Gradient-based methods*: Gradient-based methods calculate the first derivative of the objective function topology and explore the search space step by step in the direction opposite to the steepest slope (for minimization of the objective function value). Examples are the Newton-Raphson method, the Quasi-Newton method after Davidon and the Maximum-Likelihood method. This class of algorithms performs best on convex, well-posed problems, where only few steps suffice to converge to an appropriate degree. However, for a rough objective function topology, the determination of the gradient becomes error-prone, in cases the method will fail as a consequence. Problematic are furthermore the incorporation of search space restrictions and the numerical cost for calculation of the derivative for a larger amount of parameters.
- *Simplex and complex based methods*: Simplex and complex based methods also attempt to move “down slope” the objective function topology. In contrast to the gradient-based methods, this approach avoids calculation of the derivatives and the respective disadvantages. Yet, for too rough topologies, this approach will fail as well. Furthermore, the local characteristic of this method predominates. One example for this class is the Simplex-Nelder-Mead algorithm.
- *Population-based methods*: Methods of this category use a set of individuals – each representing a parameter value assignment – and employ paradigms known from the

nature with regard to the interaction of those individuals. Examples are genetic algorithms (GA), evolutionary methods (EA) and Particle-Swarm-Optimizer (PSO). Advantages are the high robustness and a relative high efficiency even for problems with many unknown parameters.

- *Topology replacement and approximation methods*: The basic idea of the topology replacement and approximation methods is a local or global approximation of the objective function topology. The extreme value search can than be temporarily performed on this substitute. Examples are adaptive response surface methods, Kriging, Moving Least Squares, and Artificial Neural Networks (ANN). These methods benefit from the fact that the optimization using the replaced surface is very fast because of the short time span necessary to compute the (approximate) objective function value. Clearly, as a nontrivial task, the way how to determine the substitute topology has to be considered.
- *Combining methods*: The category on combining methods comprises methods using a mix of the paradigms mentioned before. Examples are the Shuffled Complex Evolution method (SCE) and the Evolutionary Annealing-Simplex algorithm (EAS). With an appropriate combination of known strategies these methods are usually robust and exhibit a high efficiency.

In view of the objectives given in the motivation, a modification of the Moving Least Squares method should be given in this paper.

3 Modification of the Moving Least Squares

3.1 The Moving Least Squares Method

The Moving Least Squares method is commonly used for the generation of solid surface models for point clouds, e.g. accruing by scans of objects done by laser scanners. Because the reconstruction of objective function topologies can be treated as a similar problem, the application of this method seems a reasonable strategy. The Moving Least Squares approach is based on the works of SHEPARD 1968 and MCLAIN 1976 and was used by LANCASTER & SALKAUSAS 1981 for mesh-free approximation of highly non-linear distributed sampling points. This method can directly be applied to *n*-dimensional problems, if a scalar value is assigned to the sampling points. (MCLAIN 1976, LANCASTER & SALKAUSAS 1981, LEVIN 2003, NEALEN 2004)

The underlying idea of the MLS method is the assignment of a local approximation function $\tilde{f}_l(x)$ to each of the *k* known sampling points. The approximate function given in Equation (1) assigns to an input value x the weighted sum of k local functions, where the weighting functions θ_l are defined depending on the distance r of the value x from the position of sampling points x^l. The side condition from Equation (2) guides the choice of the local approximate functions as well as the weighting functions. Essentially, those have to be tuned in order to make the overall approximate function coincide with the prescribed values at the given sampling points. (MCLAIN 1976, LEVIN 2003, NEALEN 2004)

(1) $$\tilde{f}(x) = \sum_{l=1}^{k} \left\{ \tilde{f}_l(x) \cdot \theta_l(r) \right\} \text{ with } r = \left\| x - x^l \right\|_2$$

(2) $$\min \sum_{l=1}^{k} \left\{ \left[\tilde{f}(x^l) - f(x^l) \right]^2 \cdot \theta \left\| x - x^l \right\|_2 \right\}$$

Most frequently, constant, linear or quadratic functions are used as local approximate functions since their parameters can be easily determined from the according sampling point and its closest neighbours. A common constraint for the weighting function is that it yields positive values for all $r \geq 0$, has the greatest value for r=0, and decreases sufficiently quickly to zero for $r \to \infty$, in order to prevent a distortion of the values at other sampling points.
Equations (3), (4), and (5) display three frequently used weighting function, the range of which can be adjusted through the parameter ε.

(3) $$\theta_l(r) = \exp(-\varepsilon^2 r^2)$$

(4) $$\theta_l(r) = \frac{1}{\varepsilon^2 + r^2}$$

(5) $$\theta_l(r) = \frac{1}{\sqrt{1 + \varepsilon^2 r^2}}$$

As a positive feature of MLS methods we find that they are not predetermined by a fixed number of degrees of freedom but the latter are controlled indirectly by the available base data (i.e. the sampling points). There are numerous publications in MLS methods. For example, LEVIN 2003 and KOLLURI 2005 investigate diverse well-known local approximate functions and suggest alternatives to them. Moreover, FRANKE 1982, FASSHAUER & ZHANG 2004 and 2007, as well as MOST ET AL. 2006 discuss different weighting functions and the choice of the according control parameters.

3.2 Modification

In order to facilitate the mathematical definition of the local approximate function $\tilde{f}_l(x)$, of the weighting functions θ_l and of the according control parameters, we stipulate the formula for calculating the value of the overall approximate function $\tilde{f}(x)$ for the input value x as given by Equation (6). Thereby, we obtain that the sum of all weighting functions evaluates to 1 for every x. Note that this equation can equivalently be transformed into the form given by Equition (1), hence this modification complies with the original MLS approach.

$$\tilde{f}(x) = \frac{\sum_{l=1}^{k} \theta_l(x) \cdot \tilde{f}_l(x)}{\sum_{l=1}^{k} \theta_l(x)} \tag{6}$$

Thereby, the *k* weighting functions $\theta_l: \Omega \rightarrow \Re^+$ assign a nonnegative real number to every parameter value setting within the search space. Moreover, the value $\theta_l(x)$ controls, how strongly the local approximate function $\tilde{f}_l$ contributes to the global approximate function $\tilde{f}$ if evaluated for the input x. Fig. 2 visualizes the underlying principle of our approach. We now proceed by specifying the necessary criteria for the employed functions $\tilde{f}_l$ und θ_l:

- Coincidence of the local approximate functions with the respective sampling points: $\tilde{f}_l(x^l) = f(x^l)$. This criterion is a natural consequence of the underlying idea to approximate the objective function by $\tilde{f}_l$ for input values close to x^l.
- With increasing radial distance from the respective sampling point x^l, the weighting function is monotonic decreasing, i. e., $r_1 < r_2$ implies $\theta_l(x^l + \upsilon r_1) \geq \theta_l(x^l + \upsilon r_2)$ for all positive reals r_1 and r_2 and arbitrary vectors $\upsilon \in \Omega$ in the search space.
- In order to guarantee the coincidence of the global approximate function with the given base data (namely $\tilde{f}(x^l) = f(x^l)$ for every x^l) two alternative criteria can be posed:
  - A pole of the weighting function θ_l at the respective sampling point x^l, according to Equation (7). If this condition is fulfilled, the contributions of all other local approximate functions are reduced to zero for $x \rightarrow x^l$. The discontinuities in the function $\tilde{f}$ resulting therefrom can be removed by setting $\tilde{f}(x^l) = f(x^l)$. Moreover the global function remains continuous, if all local functions $\tilde{f}_l$ are continuous on Ω and every θ_l is continuous on $\Omega/\{x^l\}$.

    $$\lim_{x \rightarrow x^l} \theta_l(x) = +\infty \tag{7}$$

  - Complete decay of the weighting functions: $\theta_l(x^j) = 0$ for all $l \neq j$ with $l = 1 \ldots k$. An advantage of this criterion is that the sampling points do not have to be treated separately. On the other hand, in this case, it might be problematic to ensure that the

global approximate function remains well-defined for the whole search space Ω (or at least for a reasonable part $T \subseteq \Omega$ like e.g. within the area spanned by the sampling points). To achieve this, the sum in Equation (8) has to be greater than zero for all $x \in T$ which means that there must be no x such that the according values of all weighting functions are zero.

(8) $$\sum_{l=1}^{k} \theta_l(x)$$

- Depending on the applied optimization method, the global approximate function has to comply with more conditions with respect to continuity or differentiability. For example, if the function can be differentiated, one can dispense with the costly numerical calculation of the gradient and directly use the analytical derivation instead.

In order to meet the aforementioned conditions, we decided to use second-order hypersurfaces, the coefficients of which are determined via a regression. Second-order hypersurfaces prove to be adequate because they enable a non-linear approximation of the sampling point's neighbourhood without causing unwanted side effects – like oscillations in the case of Fourier analysis. The use of second-order hypersurfaces within the context of the Moving Least Squares approach has been reported on several times e.g. in McLain 1976, Most 2006, Lancaster & Salkausas 1981 and Levin 1998.

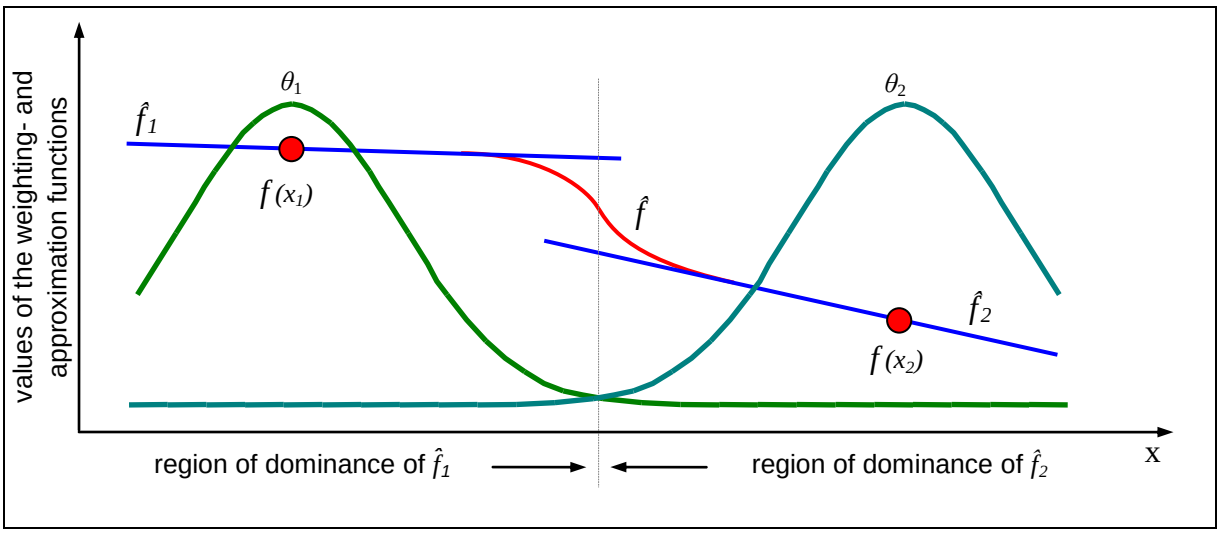

Fig. 2: Schematic of the underlying principle of weighting functions

In our approach, the weighting functions, representing the second ingredient for the Moving Least Squares method, are based on a Voronoi diagram derived from the sampling points. Fig. 3 displays a schematic of such a Voronoi diagram in $\Re^2$ including a triangulation of the

sampling points and the according Voronoi regions. Since this kind of diagrams can be easily generalized to more dimensions and efficient algorithms for their calculation are known, it is possible to use Voronoi diagrams to cover the entire search space Ω with simplices based on the available sampling point data. The neighbourhood Y_k of a sampling point k is now defined as the set of all simplices S_l which contain the same sampling point: $Y_k = \{S_l \mid x^k \in S_l\}$. This technique for stipulating the areas of influence – already described by McLain 1976 – ensures that the weighting functions gradually reduce to zero within this neighbourhood. Given an input x, the according weight for the local function corresponding to the sampling point l can be calculated via Equation (9) using the smooth step funktion (Krüger 2002) displayed in Equation (10). Due to the aforementioned property of the weighting functions of completely decaying within the given neighbourhood Equation (9) only depends on the neighbourhood containing x.

$$\theta_l(x) = \prod_{x^i \in Y_k} \left[1 - s\left(\frac{(x^i - x^l)\cdot(x - x^l)}{(x^i - x^l)\cdot(x^i - x^l)} \right) \right] \tag{9}$$

$$s(x) = \begin{cases} 0 & \text{if } x < 0 \\ 1 & \text{if } x > 1 \\ 3x^2 - 2x^3 & \text{otherwise} \end{cases} \tag{10}$$

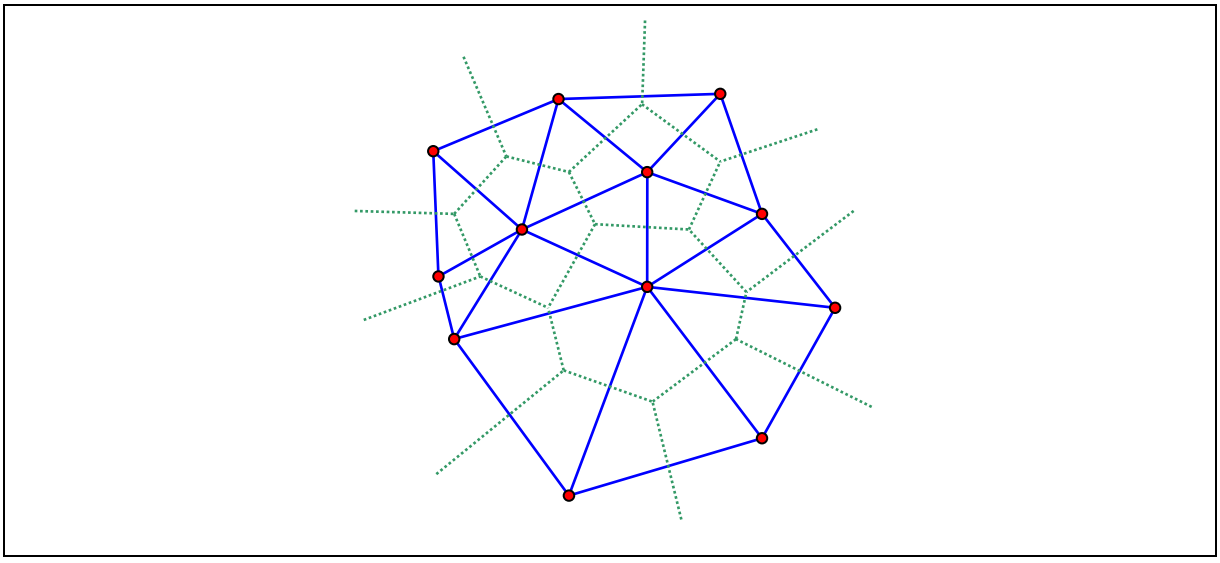

Fig. 3: Schematic of a Voronoi diagram in $\Re^2$

red points: sampling points; solid blue lines: triangulation of the point cloud; doted green lines: Voronoi-Regions

4 Validation and Application

4.1 Example 1: Mathematical Test Functions

For testing the capabilities and properties of optimization algorithms, several authors suggested standard test functions. Those test functions are used to define the objective function topology directly. Employing these test functions for validation and verification of the proposed modification of the moving least squares method has several advantages. On one hand, it takes next to no time to compute the objective function values. Furthermore, unfavorable influences from external forward calculation can be excluded.

In our first example, our proposed modification will be evaluated against the following standard test functions:

- RASTRIGIN's test function,
- ROSENBROCK's test function,
- „Moved Axis Parallel Hyper-Ellipsoid" test function

RASTRIGIN's Function

A common used test function is RASTRIGIN's test function given by Equation (11). This function depends on the first function of the DE JONG's Test-Suite (DE JONG 1975) and is based on a quadratic function added to a cosine-modulation. Because of this configuration, local optima are periodically distributed. The global optimum $f(x^*) = 0$ is located at $x_i^* = 0$ with $i = 1 : n$. This function is applicable to an arbitrary number of unknown variables.

$$f(x) := 10 \cdot n + \sum_{i=1}^{n} \left(x_i^2 - 10 \cdot \cos(2 \cdot \pi \cdot x_i) \right) \quad f(x^*) = 0;\ x_i^* = 0;\ i = 1 : n \tag{11}$$

Fig. 4 shows in the upper part the original shape of RASTRIGIN's test function for two parameters both having a range of [-1 … 1]. The lower part contains the visualization of the approximated objective function topology on the basis of a 6 x 6 raster. The raster shows the minimal function value for 4 points with coordinates (-0.16; -0.16), (0.16; -0.16), (-0.16; 0.16) und (0.16; 0.16). As the figure shows, the approximation function is capable of emulating the shape of the original RASTRIGIN's test function very well on the basis of the 36 sampling points.

Because of the missing information outside of the region spanned by the sampling points, the approximation shows large aberrations and apparent extreme values there. For an unconstrained subsequent optimization procedure, these artifacts may have negative effects. With respect to this observation, it seems to be beneficial to restrict the search range of

subsequent optimization procedures by 5 to 10% compared to the area covered by the sampling points.

Fig. 5a shows the results of an optimization on the approximated topology with a Particle Swarm Method with 10 individuals (EBERHARDT & KENNEDY 1995, KENNEDY & EBERHARDT 1995, SHI & EBERHART 1998a and 1998b, VAN DEN BERG 2001). Already after 4 calculation steps (40 forward calculations), the algorithm identifies (5.928E-003; 1.292E-002) as best solution vector. As shown in Fig. 5b, a similar effect can be achieved by the used gradient method (modified and damped Newton–Raphson method; PRESS et al. 1992): after just 8 calculation steps (40 forward calculations) this method – started from (0.4; 0.4) – reaches the solution vector (4.250E-004; 4.241E-004).

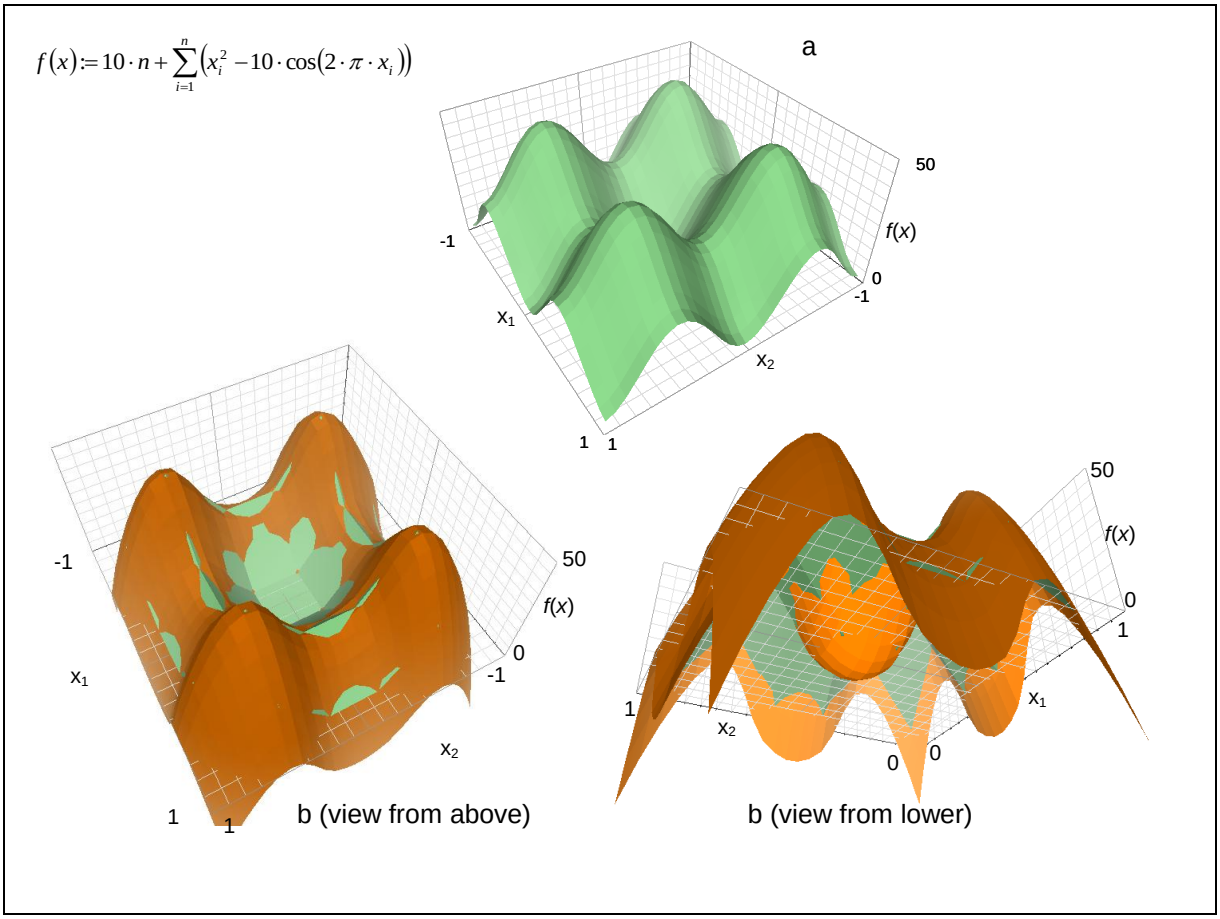

Fig. 4: original shape (above) and two views of the approximation of the RASTRIGIN's test function for two parameters on the basis of a 6 x 6 raster (green: 6 x 6 raster; orange: approximation)

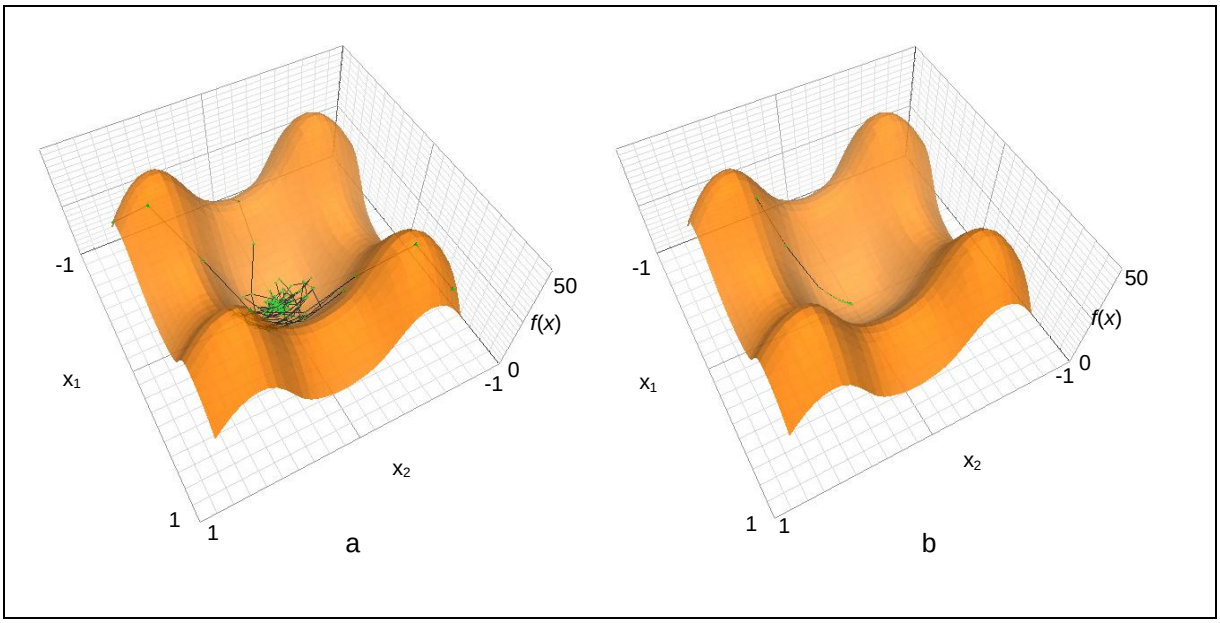

Fig. 5: Optimization results for the modified MLS-method for RASTRIGIN's test function for two parameters on the basis of a 6 x 6 raster (left: Particle-Swarm-Optimizer; right: gradient method)

ROSENBROCK's test function

ROSENBROCK's test function – also known as „Banana function"– has primarily been defined for 2 dimensions. According to formula (12), this function can be easily generalized to an arbitrary number of parameters (POLHEIM 1999). The global optimum is located at $f(x^*) = 0$ with $x_i^* = 1$ and $i = 1 : n$. Fig. 6 shows the function for two parameters in range [-2…2].

(12) $$f(x) := \sum_{i=1}^{n-1} 100 \cdot \left(x_{i+1} - x_i^2\right)^2 + \left(1 - x_i\right)^2$$

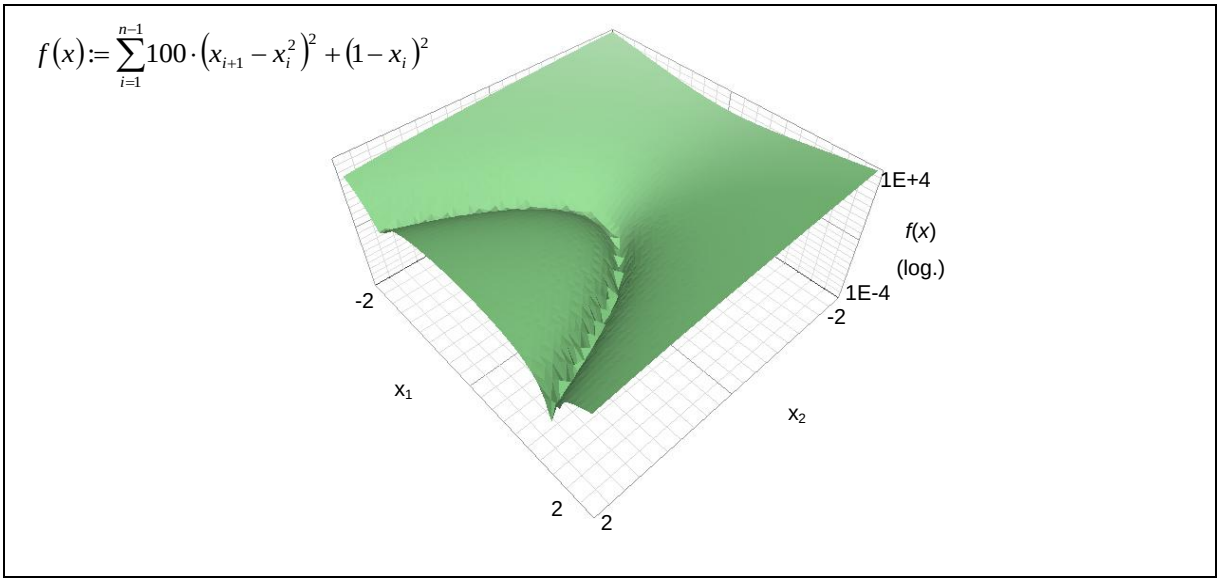

Fig. 6: ROSENBROCK's test function for two parameters in range [-2…2]

The approximation of ROSENBROCK's test function for two parameters in range [-2…2] on the basis of a 6 x 6 raster and a 7 x 7 raster is shown in Fig. 7. For the 6 x 6 raster, the global optimum is represented by chance by one sampling point at (1; 1). According to this the approximation shows this extreme value, too. Anyway, the "elongated valley" of ROSENBROCK's test function is obviously also captured quite well by the approximation, so that the search range for the global optimum can be easily restricted even without the sampling point at (1; 1). The "inequalities" of the valley are due to the small number of sampling points. Avoiding the "lucky strike" of the 6 x 6 raster, Fig. 7b shows the results of the 7 x 7 raster. The best sampling point of this raster is located at (0; 0). The visualization of the approximated topology shows a picture very similar to Fig. 7a: an arched shape of the valley is clearly shown and extreme values are only shown within the valley.

When applying optimization methods with varying starting parameters to the obtained approximating hypersurfaces, the three optima recognizable in Fig. 7 were found in several runs.

Because of the relatively low temporal and computational effort of the optimization on the approximation, several independent optimization runs are unproblematic. The determined solutions vectors can be checked with the "real" forward calculation. If applicable, they can be added to the existing sampling points and be a basis for new – and obviously more precise – approximation.

Moved Axis Parallel Hyper-Ellipsoid test function

The not so well-known *Moved Axis Parallel Hyper-Ellipsoid* function is especially suited for demonstration purposes, because the global optimum shows for each parameter a different value ($f(x^*) = 0$ with $x_i^* = 5i$ and $i = 1 : n$). This function is based on a hyperellipsoid parallel to the coordinate system axes (POLHEIM 1999). The test function definition is shown in Equation (13). Fig. 8 (left) displays a visualization of the function.

$$f(x) := \sum_{i=1}^{n} \left(i \cdot (x_i - 5i)\right)^2 \quad f(x^*) = 0;\ x_i^* = 5i;\ i = 1:n \tag{13}$$

With this test function, the performance of a selection of optimization algorithms should be compared to the results of our modified Moving Least Squares method for the 2D case. This comparison uses as criterion the geometrical distance of the best solution to the global optimum at (5; 10). Fig. 8 (right) shows a typical history diagram of the deviations and the distance to the global optimum depending on the needed forward calculation calls of a particle swarm optimizer (PSO; EBERHARDT & KENNEDY 1995, KENNEDY & EBERHARDT 1995, SHI & EBERHART 1998a and 1998b, VAN DEN BERG 2001), a gradient descent method

(modified and damped Newton–Raphson–Method; PRESS et al. 1992) and a evolutionary algorithm (SCHILLING 2003). For a correct interpretation of these diagrams, note that 10 calls of the forward calculation per optimization step will be needed by the PSO and evolutionary algorithm.

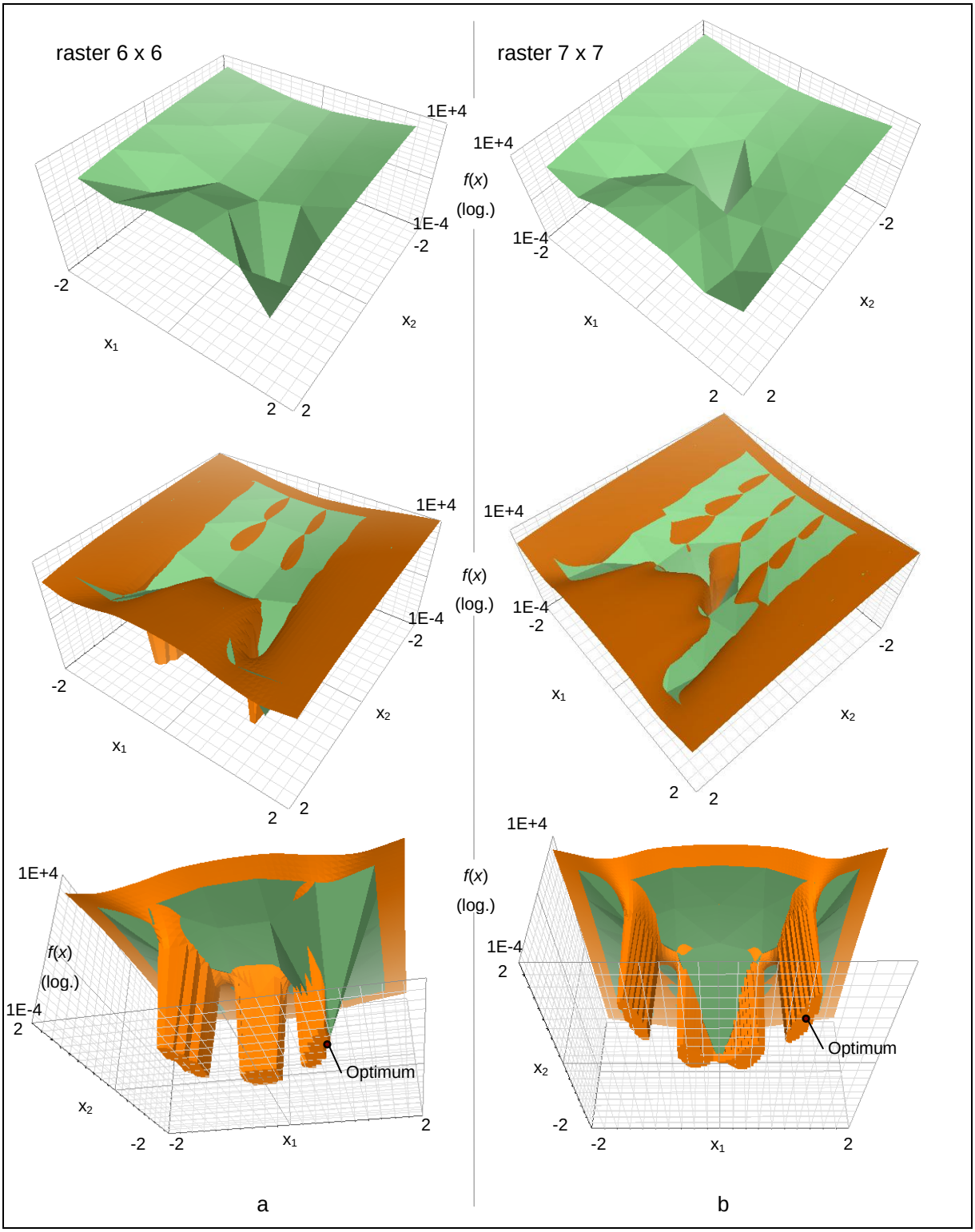

Fig. 7: Approximation of ROSENBROCK's Function for two parameters in range [-2…2] based on a 6 x 6 raster (left) and a 7 x 7 raster (right)

In result, the PSO needed 90 calls to reach a geometrical distance to the global optimum smaller than 1.0. The gradient method needed 50 calls and the evolutionary algorithm 90 calls. In Tab. 1, the calculation costs are summarized.

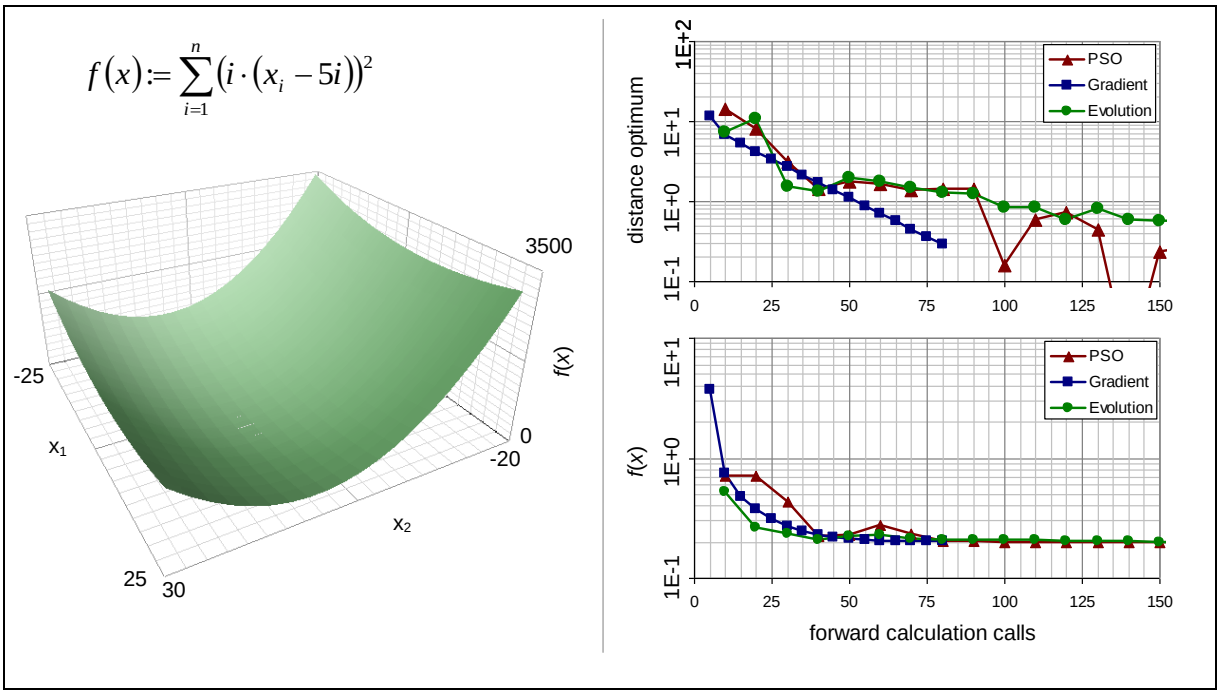

Fig. 8: *Moved Axis Parallel Hyper-Ellipsoid* function for two parameters with range [-25…25] respectively [-20…30] and history of different optimization algorithms

With respect to the simple objective function topology, a 4 x 4 raster was used as basis for the approximation. When searching for the optimum on the approximated hypersurface, a recursive raster method (where after each run, the search area is restricted to the best cell and its neighbours) yields (4.977, 9.977) after the third recursion (remaining distance to optimum: 0.03), while a PSO method with 10 individuals obtains (5.096, 9.972) after 30 calculation steps (distance 0.1). Consequently, the modified MLS method arrives at a more precise result using only 16 sampling points, hence performing better than established methods which additionally need more calls of the original objective function.

For the case of the *Moved Axis Parallel Hyper-Ellipsoid* function with three parameters, a 4 x 4 x 4 raster was chosen as basis for the modified Moving Least Squares method. Also this example could be solved by our method without problems.

Tab. 1: Comparison of the results for the *Moved Axis Parallel Hyper-Ellipsoid* function (number of calculation steps respectively forward calculation calls for reaching a geometrical distance smaller than 1.0 to the global optimum)

Method	calculation steps	forward calculation calls
Gradient based method	10	50
evolutionary method	9	90
particle swarm optimizer	9	90
modified moving least squares	~	16

The sufficiency of a low number of sampling points as demonstrated here can only be assumed, if the objective function topology is accordingly smooth. If the complexity or the number of involved parameters increases, larger numbers of sampling points will be needed to obtain a reliable approximation. Also, ideally, these sampling points should be chosen such that they are "representative" for the search space. Therefore, in the example presented here, we chose a simple raster-based method because it homogenously covers the given area. However, other methods such as Latin Hypercube could be applied as well.

Conclusions for example 1

Based on the three test functions from Example 1, we have shown that the modification of the moving least square method is able to approximate the shape of an objective function topology. As a result, this method can be used to accelerate the finding of extreme values. In summary, the following statements are derived:

- Outside the area covered by the sampling points, the approximate surfaces might exhibit extrema that are not present in the original function. Hence, reliable propositions about extrema of the underlying objective function can only be made for the interior of this sampling region. This has to be taken into account when choosing the sampling points.
- As a result of the approximation, connected extremal regions of the original function might result in several disconnected regions of the approximate function. As calculations on the approximate functions can be done comparably fast, several runs with varying initial values can be carried out in order to not miss parts of those extremal regions.
- Preferably, the used sampling points should cover the search space in a representative way and take into account the number of parameters and possible information about the objective function topology. For the generation or completion of according sampling data,

Latin Hypercube and (in case of small numbers of parameters) raster methods have proven to be beneficial.

- A quality check of the approximated topology can be done by a comparison of the approximated value and the value of a forward calculation with given parameter vectors. Of course, those testing parameter vectors must not have been used for generating the approximating hypersurface. Also functions of higher degree can be used in order to obtain a better approximation behaviour. However, this might be at the cost of other pleasant properties: more input data is needed for a regression, the extrapolation capabilities might degrade even more and their might be disadvantages with respect to the functions' analytical properties (e.g. for the analytical calculation of the gradient).

4.2 Example 2: Back analysis of weathered zone depth using inclinometer readings

In the sequel, we will discuss how our method can be employed to determine the boundary between weathered and non-weathered zones of a slope based on data from surface displacement measurements or data from synthetic inclinometers. The numerical model of the slope with the instrumented two inclinometers is depicted in Fig. 9. Loading to the slope has been realized by adding and consequently excavating a layer of material filling the valley at the slope's toe. The slope is supposed to consist of two layers and the material composing the upper layer is considered to be weathered. The next assumption in the model is that the material properties of the weathered material increase with the depth as linear function of the distance from the slope surface. At the boundary between weathered and non-weathered materials we assume a continuity of the material properties. Schematically, the setting is given in Fig. 9 as distribution profile of the selected material parameters. A 2D model of the considered slope has been built in the finite element software ABAQUS/Standard. The used mesh and the boundary conditions for the geostatic equilibrium step are shown in Fig. 10. The boundary condition at the bottom of the model has been modified for the consequent calculations steps and no horizontal displacements were allowed, thereby modeling the contact with possibly very rough rock base surface.

The filling material of the layer above the toe valley is excavated by ramped in time elevating of the whole piece and this way quasistatic unloading of the slope is modeled. The resulting displacements are returned to be compared with inclinometer readings and this way the solution of the forward problem serves as objective function for the optimization procedure.

The material model chosen for this example slope comprises linear elasticity and Mohr-Coulomb plasticity. The filling material of the layer imposing the load on the toe of the slope is taken to be linear elastic. The material model parameters listed in Tab. 2 are used for gaining synthetic data for the consequent back analysis.

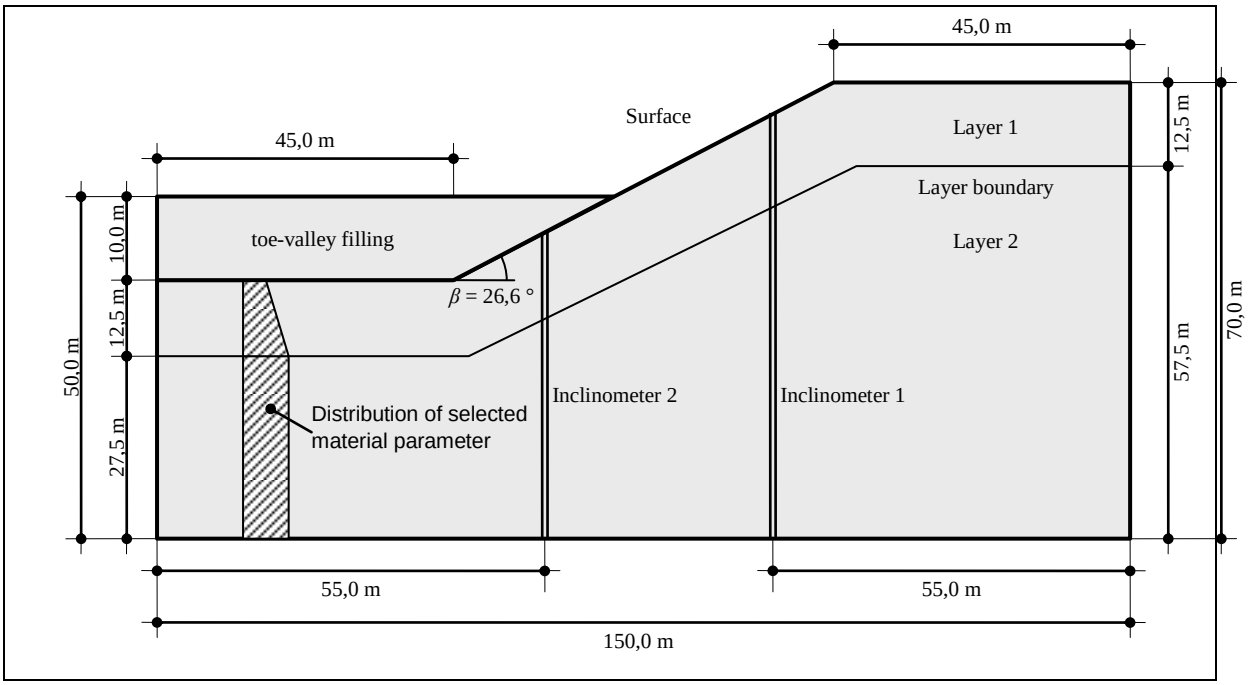

Fig. 9: The model for a numeric experiment of releasung the slope toe-valley filling

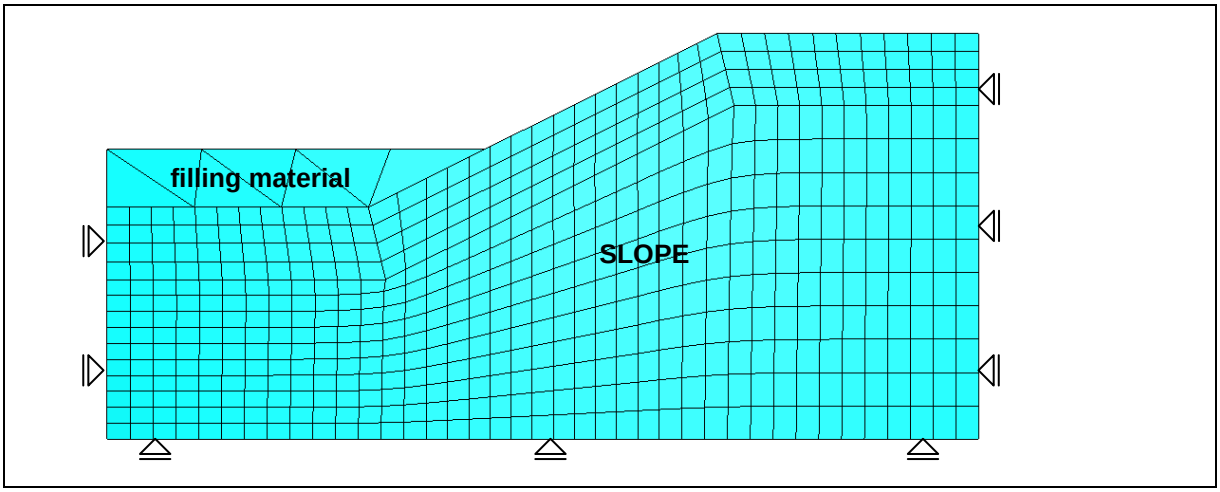

Fig. 10: FE mesh and boundary conditions for the step of filling material removal

Tab. 2: Material parameters of the reference simulation

Parameter	Unit	Value for synthetic data	Trusted zone
Slope			
density	[kg/m³]	2200	
Young's modulus at the surface E_{surf}	[N/m²]	1E+08	
E_{nw}	[N/m²]	7E+08	5E+08 to 1E+09
Poisson's ratio v	[-]	0.3	
friction angle φ_{nw}	[°]	30	25 - 35
friction angle φ_{surf}		30	
cohesion c	[N/m²]	1E+04	
depth of layer boundary t	[m]	12.50	7.5 to 17.5
toe valley filling			
Density	[kg/m³]	2200	
Young's-modulus E	[N/m²]	7E+09	
Poisson's ratio v	[-]	0.3	

This section presents the back analysis of the weathered zone depth and the material parameters of the non-weathered layer using the known material parameters at the slope surface and the measured displacements by two inclinometers. There are three parameters of the model to be identified: the values of Young's modulus (E_{nw}) and the friction angle (φ_{nw}) for the non-weathered material and the depth of the weathered zone (t). The trusted zone for the parameters to be back calculated is defined by the given in Tab. 2 constrains. The merit function $f(x)$, which has to be minimized, relates the measured and calculated displacements. The definition of the objective function is based on the least-squares fit and is shown by Equation (14). This function compares the displacements at q given locations within a defined time interval (calculation step).

$$f(x) := \sqrt{\frac{1}{q}\sum_{p=1}^{q}\left(u_{p,\,x,\,calc} - u_{p,\,meas}\right)^2} \tag{14}$$

Six different sets of parameters have been used for the procedure. Sets 1 and 2 use the measured displacements at the top of inclinometer 1 and inclinometer 2, respectively (see Fig. 9). Set 3 combines set 1 and set 2. Sets 4 and 5 use the displacements along the inclinometer 1 or inclinometer 2 respectively and set 6 is composed of the displacements at all nodes along the both inclinometers. Fig. 11 presents a subsection of the objective function for sets 3 and 6. When comparing the two subsections shown in Fig. 11, it is evident that for set 3 (Fig. 11b) the objective function is less smooth and the log deviation varies within a larger interval. This fact influences the calculation cost for obtaining the best fit.

The report for the optimization runs using sets 3 and 6 is given in Tab. 3. For the optimizations, the least-squares fit was used and for the minimum search the particle swarm algorithm with ten individuals (EBERHARDT & KENNEDY 1995) were applied directly, respectively on the approximation surface. In case of data set 6 the searched minimum at (E_{OM} = 7.001E+008 N/m²; t = 12.49 m; φ = 30.0°) in found by an PSO with 10 individuals usually after 35 to 40 calculation steps. If only data set 3 is available for the objective function, the particle swarm optimizer needs usually about 50 to 55 calculation steps. For set 1 or 2, no reliable inverse determination of the tree parameters are possible: Neither of the used optimization algorithms was able to converge. The reason for this is the existence of non-uniqueness of the inverse problem. In further calculations, we found that the number of computation steps for obtaining the best fit decreases when adding data to the merit function.
For the modified Moving Least Squares method of this three-dimensional problem, 75 sampling points generated by a Latin Hypercube method were used. For comparison: a simple 6 x 6 x 6 raster already contains 216 sampling points and therefore 216 forward calculation calls would be required. A PSO with 10 individuals required 20 calculation steps for the approximation of the optimum (E_{OM} = 6.965E+008 N/m²; t = 10.6 m; φ = 29.9°) based on the complete data sets of one or both inclinometers. The already mentioned roughness of the objective function based on the measurements caused an additional "virtual" extremum at. (E_{OM} = 6.600E+008 N/m²; t = 8.9 m; φ = 28.9°). However, the real optimum was found in approximately 75 % of the PSO runs on the approximate function.

Tab. 3: Comparison of the computation costs for obtaining the best fit

Reference data	Calculation steps	Function calls
Data set 6: particle swarm optimizer	35 to 40	350 to 400
Data set 6: modified moving least squares	~	75
Data set 3: particle swarm optimizer	50 to 55	500 to 550
Data set 3: modified moving least squares	~	75

Conclusions for example 2

Reviewing on the calculations of Example 2, it could be shown that the proposed method is also applicable to problems with a higher topology roughness. Especially for complex numerical simulations, these types of objective function topologies have to be expected. Furthermore, we demonstrated that this method can be used for more than two unknown model parameters.

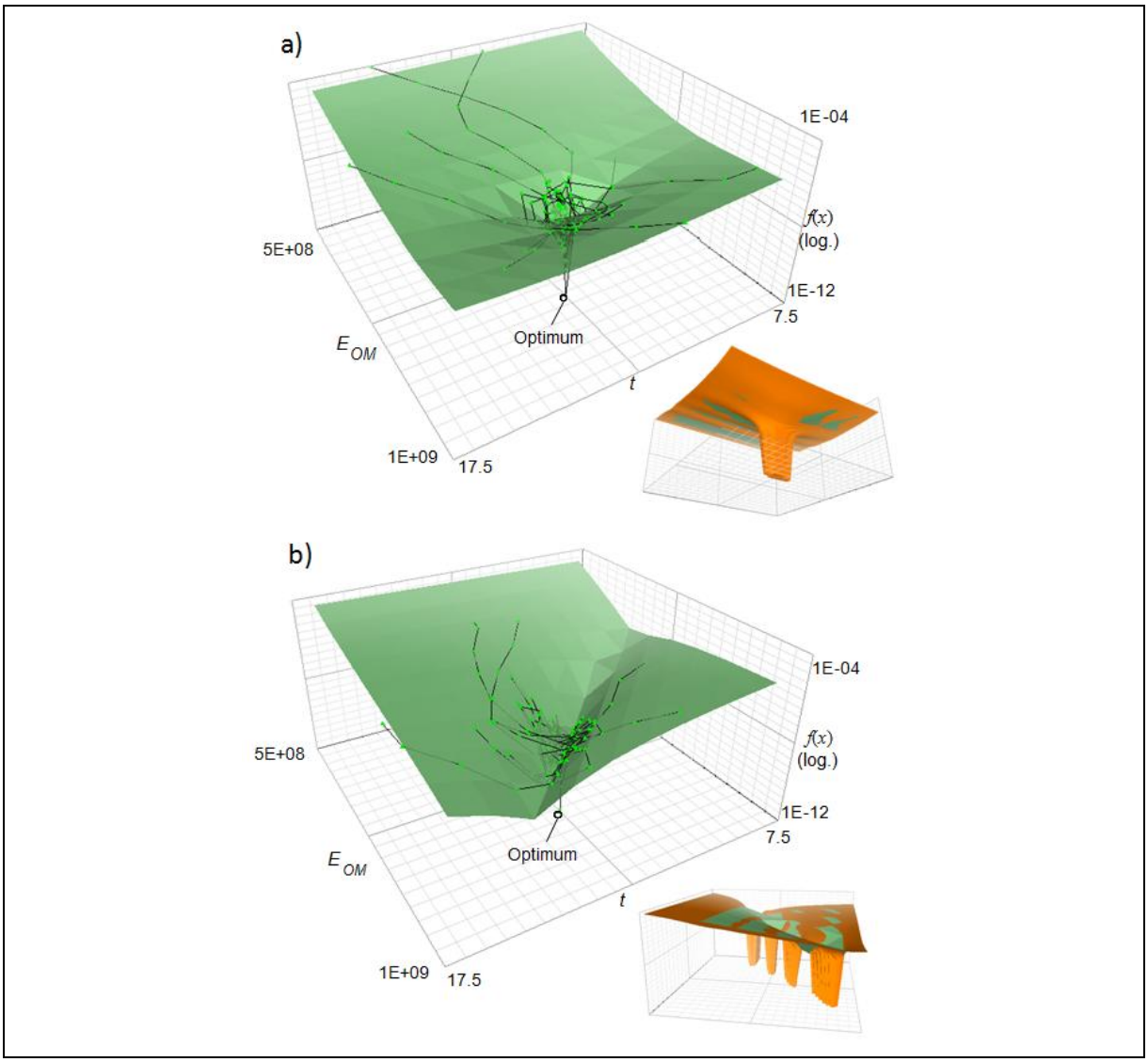

Fig. 11: Partial plots of the objective function a) using set 6; b): using set 3.

5 Conclusion

With the presented modified Moving Least Square method, we proposed a powerful and accelerated optimization algorithm and demonstrated that our method is allows to reduce the number of forward calculations significantly, being of utmost importance dealing with complex tasks in the field of civil engineering. The basic idea of this procedure is to avoid expensive forward calculation calls by using a (computationally and analytically) less costly proximity function instead. The search for the extremum is then done by using the approximate function instead of the original objective function.

It should be mentioned however, that our method does not represent a panacea for accelerating or solving optimization problems. Naturally, in the presented setting, the results cannot be better than both the input data as well as the used optimization method. However, the elaborated evaluation of the available data usually leads to an improved approximation of

the extrema and a faster convergence. Moreover, the use of approximation by hypersurfaces is not restricted to optimization problems or to the context of inverse determination of model parameters. Other potential application domains are graphical representation of data structures as well as reconstruction of missing data. Our future work will be particularly focused on performance improvements for problem settings involving a higher number of dimensions. .

Acknowledgements

The first author acknowledges the support by the German Research Foundation (DFG) via the projects SCHA 675/7-2 and SCHA 675/11-2 ("Geomechanical modelling of large mountainous slopes").

Literature

VAN DEN BERG, F. (2001): An Analysis of Particle Swarm Optimizers. PhD thesis, University of Pretoria.

BIALY, H.; OLBRICH, M. (1975): Optimierung – eine Einführung mit Anwendungsbeispielen. VEB Fachbuchverlag Leipzig, 1. Auflage.

BITTERLICH, S.; KNABNER, P. (2002): An Efficient Method for Solving an Inverse Problem for the Richards Equation. Institute for Applied Mathematics, Friedrich-Alexander Universität, Erlangen-Nürnberg.

BOYD, S.; VANDENBERGHE, L. (2006): Convex Optimization. Cambridge University Press.

CALVELLO, M.; FINNO, R. J. (2002): Calibration of soil models by inverse analysis. In Pande & Pietruszczak (eds.): Numerical Models in Geomechanics NUMOG VIII, Balkema, Rotterdam, pp. 107 - 116.

CARRERA, J.; ALCOLEA, A.;MEDINA, A.; HIDALGO, J.; SLOOTEN, L. J. (2005): Inverse problem in hydrogeology. Hydrogeological Journal 13, Springer-Verlag, S. 206 – 222.

DE JONG, K. (1975): An analysis of the behaviour of a class of genetic adaptive systems. PhD thesis, University of Michigan.

EBERHARDT, R. C.; KENNEDY, J. (1995): A new optimizer using particle swarm theory. Proceedings of the Sixth International Symposium on Micro Machine and Human Science, Nagoya, Japan, IEEE Service Center, Piscataway, NJ, 39 – 43.

FASSHAUER, G. E.; ZHANG, J. G. (2004): Recent results for moving least squares approximation. In M. L. LUCIAN and M. NEAMTU (editors), Geometric Modeling and Computing, Seattle, Brentwood, TN, S. 163 - 176.

FINSTERLE, S. (1998): Multiphase Inverse Modelling: An Overview. U.S. Department of Energy's Geothermal Program Review XVI, Berkeley, California.

FINSTERLE, S. (2000): Demonstration of Optimization Techniques for Groundwater Plume Remediation. Earth Sciences Division, Lawrence Berkeley National Laboratory, University of California, Berkeley.

FLEISCHER, J.; BROOS, A. (2004): Parameteroptimierung bei Werkzeugmaschinen – Anwendungsmöglichkeiten und Potentiale. Weimarer Optimierungs- und Stochastiktage 1.0, Weimar.

FLORES SANTIAGO, O.; BAUSINGER, R. (1998): Automatische Schweißpunkt-Optimierung an Karosserien. XXV. FEM – Kongress, Baden-Baden.

FRANKE, R. (1982): Scattered data interpolation: tests of some methods. Math. Comput. 48, S. 181 - 200.

HADAMARD, J. S. (1902): Sur les problèmes aux dérivées partielles et leur signification physique. Princeton University Bulletin, S. 49 - 52.

JEONG, S.-J. (2003): Ein Beitrag zur Erzeugung nichtlinearer Entwurfsseegänge im numerischen Wellenkanal. Dissertationsschrift, Fakultät für Verkehrs- und Maschinensysteme, TU Berlin.

KENNEDY, J.; EBERHARDT, R. C. (1995): Particle Swarm Optimization. Proceedings of IEEE International Conference on Neural Networks, Volume IV, S. 1942 – 1948, Perth, Australia, IEEE Service Center, Piscataway, NY.

KOLLURI, R. (2005): Provably Good Moving Least Squares. ACM-SIAM Symposium on Discrete Algorithms, S. 1008 - 1018.

KRÜGER, J. H. (2002): Echtzeitsimulation und –darstellung von Wolken. Diplomarbeit, Fachbereich Informatik, RWTH Aachen.

LANCASTER, P.; SALKAUSAS, K. (1981): Surfaces generated by moving least squares methods. Mathematics of Computation 87, S. 141 - 158.

LEVIN, D. (2003): Mesh-Independent Surface Interpolation. In: “Geometric Modeling for Scientific Visualization" Edited by Brunnett, Hamann and Mueller, Springer-Verlag, S. 37 - 49.

LEVIN, D. (1998): The Approximation Power of Moving least Squares. Mathematics of Computation, Vol. 67, Nr. 224, S. 1517 - 1531.

LOUIS, A. K. (1989): Inverse und schlecht gestellte Probleme. Teubner-Verlag, Stuttgart.

MATOUŠ, K.; LEPŠ, M.; ZEMAN, J.; ŠEJNOHA, M. (2000): Applying genetic algorithms to selected topics commonly encountered in engineering practice. Computer methods in applied mechanics and engineering 190, Elsevier, S. 1629 - 1650.

MCLAIN, D. H. (1976): Two dimensional interpolation from random data. The Computer Journal, Vol. 19, S. 178 - 181.

MEIER, J.; SCHÄDLER, W.; BORGATTI, L.; CORSINI, A.; SCHANZ, T. (2008): Inverse Parameter Identification Technique using PSO Algorithm Applied to Geotechnical Modeling. . Journal of Artificial Evolution and Applications, http://www.hindawi.com.

MOST, T. (2006): A natural neighbor based moving least squares approach for the element-free Galerkin method. International Journal for Numerical Methods in Engineering, Vol. 71, Issue 2, S. 224 - 252.

MOST, T.; BUCHER, C.; MACKE, M. (2006): A natural neighbor based moving least squares approach with interpolating weighting function. 17th International Conference on the Application of Computer Science and Mathematics in Architecture and Civil Engineering, K. Gürlebeck & C. Könke (eds.), Weimar.

NEALEN, A. (2004): An as-short-as-possible introduction to the least squares, weighted least squares and moving least squares methods for scattered data approximation and interpolation. Technical report, Discrete Geometric Modeling Group.

POLHEIM, H. (1999): Evolutionäre Algorithmen – Verfahren, Operatoren und Hinweise für die Praxis. Springer.

PRESS, W. H.; FLANNERY, B. P.; TEUKOLSKY, S. A.; VETTERLING, W. T. (1992): Numerical Recipes in C: The Art of Scientific Computing. Cambridge University Press; 2. Auflage.

SCHANZ, T.; ZIMMERER, M.; DATCHEVA, M.; MEIER, J. (2006): Identification of constitutive parameters for numerical models via inverse approach. Felsbau- Rock and Soil Engineering, Volume 25, No. 2, 11-21.

SCHILLING, S. (2003): Beitrag zur Lösung ingenieurtechnischer Entwurfsaufgaben unter Verwendung Evolutionärer Algorithmen. Dissertationsschrift, Fakultät Bauingenieurwesen, Bauhaus-Universität Weimar.

SCHLEGEL, R.; WILL, J. (2006): Parameteridentifikation und Sensitivitätsanalyse zur Ermittlung relevanter Bauwerksbereiche für die Materialprüfung bei historischen Mauerwerkstrukturen. DYNARDO GmbH.

SHEPARD, A. (1968): A Two-Dimensional Interpolation Function for Irregularly Spaced Points. Proceedings A.C.M National Conference 1968, S. 517 - 524.

SHI, Y.; EBERHART, R. C. (1998b): A modified particle swarm optimizer. Proceedings of the IEEE International Conference on Evolutionary Computation, S. 69-73. Piscataway, NJ: IEEE Press.

SHI, Y.; EBERHART, R. C. (1998a): Parameter Selection in Particle Swarm Optimization. Evolutionary Programming VII: Proc. EP98, New York: Springer-Verlag, S. 591 600.

SPALL, J. C. (2003): Introduction to stochastic search and optimization: estimation, simulation and control. Wiley-Interscience series in discrete mathematics.

ZHANG, Z. F.; WARD, A. L.; GEE; G. W. (2003): Estimating Soil Hydraulic Parameters of a Field Drainage Experiment Using Inverse Techniques, Soil Science Society of America, Vadose Zone Journal, Vol. 2, pp. 201 - 211.